J. Cent. South Univ. (2014) 21: 3896−3910
DOI: 10.1007/s11771-014-2377-6

Springer

Waste heat water pumping model with direct contact cooling

Kittiwoot Sutthivirode[1], Naris Pratinthong[1], Pichai Namprakai[1], Natthaphon Roonprasang[2], Taveewat Suparos[3]

1. Division of Energy Technology, School of Energy, Environment and Materials, King Mongkut's University of Technology Thonburi, Bangkok 10140, Thailand;
2. Department of Alternative Energy Development and Efficiency Ministry of Energy, Bureau of Energy Regulation and Conservation, Bangkok 10330, Thailand;
3. Department of Mechanical Technology Education, Faculty of Industrial Education and Technology, King Mongkut's University of Technology Thonburi, Bangkok 10140, Thailand

Abstract: The performance of a patented water pumping model with steam-air power was presented, which operates automatically by direct contact cooling method. The main objective was to study feasibility of a pumping model for underground water. In this model, a heater installed within the heat tank represented sources of waste heat as energy input for finding appropriate conditions of the 10 L pump model. The system operation had five stages: heating, pumping, vapor flow, cooling, and water suction. The overall water heads of 3, 4.5, 6 and 7.5 m were tested. At the same time, it was found that the pump with 50% air volume is sufficient for pumping water to a desired level. In the experiment, the temperatures in the heating and pumping stages were 100−103 °C and 80−90 °C, respectively. The pressure in the pumping stage was 12−18 kPa, and the pressure in the suction stage was about −80 kPa, sufficient for the best performance. It could pump 170 L of water at a 2 m suction head, 120 L at a 3.5 m suction head, 100 L at a 5 m suction head, and 65 L at a 6.5 m suction head in 2 h. A mathematical model for larger pumps was also presented, which operates nearly the same as the present system. Economic analysis of the 10 L pump was also included.

Key words: direct contact cooling; driving tank; steam-air power; liquid piston; waste heat

1 Introduction

The industrial sector is a large sector that consumes a huge amount of fossil-based electrical energy. In addition to illumination, it is used for operating machines, equipment and also pumps. Pumps are necessary in industry since they are used to pump water in cooling processes, cleaning machines and the manufacturing process in some industries. In manufacturing processes, heat is released to the environment even if it still has some potential. If the heat is harnessed and reapplied into pumping tasks, world energy consumption would be reduced and the effects of global warming may become lower.

The thermal water pump was invented by SAVERY in 1690 [1], which used steam for its operation. Nowadays, pumps can be operated by thermal energy from renewable energy such as solar energy. The researches that have been performed on the heat pump, including thermodynamics by PYTILINSKI [2] and BAHADORI [3], showed the principles of solar water pumping by thermodynamic or direct-conversion methods. JENNESS and JAMES [1] considered the important characteristics of the solar-powered SAVERY water pump. HIRANO et al [4] studied the heat pipe to drive the thermal pump. SUDHAKAR et al [5] used solar water pumps for irrigation. RAO and RAO [6] developed and tested two types of solar water pump systems for irrigation. Their system was cooled by air and water. Pentane used as the working fluid was more expensive. Their system was comprised of a solar collector, flash and water tanks. It was cooled by air at night. This pump had disadvantages in the first round and limitations based on the pumped-water tank cost. The water-cooled one was superior to the air-cooled one. In the same year, SHELDON et al [7] studied the water pump system using heat energy to generate volume change of a fluid controlled by a check valve. The oscillations of the vapor-liquid in the column were the main pumping method. PICKEN et al [8] studied the development of a water piston solar-powered steam pump. They utilized the 2 m^2 solar collector (SC) comprising an evacuated tube integrated with a heat pipe. The 110 °C boiling steam was produced to pump water from a deep well. Their pump efficiency was around

Received date: 2013−12−30; **Accepted date:** 2014−05−28
Corresponding author: Pichai Namprakai; Tel: 662−02−470−8622; Fax: 662−02−470−8623; E-mail: pichai.nam@kmutt.ac.th; ipicakai@gmail.com; kittiwoot_05@hotmail.com

0.05% with the pumping rate of 10−20 L/h. The lifting heads were 2−8 m. SUMATHY [9−10] did a research on a thermal water pump with a 1 m^2 solar collector (SC). It had 0.12%−0.14% overall efficiency, 6−10 m discharge heads and 12−23 cycle/d. The 15 kg water mass was raised in each pumping cycle. WONG and SUMATHY [11−13] presented the performance of the solar water pump by using *n*-pentane and ethyl ether as the working fluids with a thermodynamic analysis to determine the optimal conditions of the solar water pump. When considering in terms of efficiency and economy, it was found that ethyl ether was the best working fluid. It had been predicted that the high efficiency would increase to 0.42%. WONG and SUMATHY [14] discussed further about research related to the solar water pump. In 2009, there were more confabulations about the heat from solar radiation driving heat engines for pumping by DELGADO-TORRES [15]. LIENGJINDATHAWORN et al [16] presented an experiment on the theory of a water pump using thermal energy (a pulsating steam water pump). The system used an electric heater to supply thermal energy for producing a steam working fluid at low temperature (90−120 °C). From the experiment, it was found that the pump efficiency was about 0.005%−0.03%, the amount of water pumping was 1−8 L/cycle and the discharge head was 1 to 2.5 m. However, the system did not operate automatically. Cooling time was still long. ROONPRASANG et al [17−18] initially constructed the solar water heater coupled with a liquid piston solar pump (LPSP). The system mainly used a 1.58 m^2 SC. The pump could operate when solar energy inputs were about 580, 600 and 630 W/m^2 for the 1, 1.5 and 2 m discharge heads, respectively. The average solar collector water temperature was between 75 and 78 °C. The mean pump efficiency was around 0.0014%−0.0019% while the LPSP powered by a heater had 0.011% efficiency. SUTTHIVIRODE et al [19] found that an LPSP powered by the sun had 0.0017% efficiency. More energy loss occurred at the SC because not all of the energy was used to produce the steam power. With the aid of air addition, the SC with low temperature could produce pressure sufficient for water pumping. KOITO et al [20] studied the characteristics of the top-heat-type long heat transport loop. The system consisted of the heat, the cooling and the reservoir sections, valve, and pipe connections. In this work, the heat source was outside the heated section. The heat was transported by use of fluid and a heat exchanger.

Recently, CHUNG et al [21] developed a new solar water heater system (SWHS) that used a solar bubble pump instead of an electric pump. The system consisted of a 2.61 m^2 heat pipe evacuated tube solar collector (HEC) with 45° inclination. The bubble pump could operate at a collector temperature of around 90−100 °C and a vapor gage pressure of 80−90 kPa. The results showed that the proposed system achieved 10% higher system characteristic efficiency than the conventional systems using electric pumps. Moreover, the former was a zero-carbon system. Other methods to produce hot water using solar energy could be found elsewhere [22−24]. More related works were discussed extensively in Refs. [25−63].

However, the pump operated by solar energy has a limitation of unstable climate that affects the rates of incident rays and the operating time because the appropriate light intensities are in the interval of 9.00 am−3.00 pm typically.

In this work, the authors aimed to develop a new pumping system that could use waste heat as a heat input of the system. The 10 L pump was tested to determine the significant parameters that affected system performance. Economic analysis of the 10 L pump was also included. In addition, a simple simulation was done for the larger driving tank that had only three stages: heating, cooling, and water suction stages. The effects of pump and suction head size were investigated.

2 Experimental setup

As shown in Fig. 1, the heat tank (HT) of 20 cm× 30 cm×5 cm was made from 0.2 cm stainless steel and was covered by aeroflex insulation (thermal conductivity of 0.040 W/(m·K)). It contained 3 L of water to produce sufficient vapor at 100 °C for the driving tank (DT). For safety, it was installed lower than the DT in order to ensure that it had adequate water every time. The DT cylinder (pump or condenser in this system) was made from stainless steel sheet with 0.2 cm thickness, 20 cm diameter and 30 cm length. The HT and DT were connected by a 1/2 inch copper tube and were covered by 5 cm insulation. The storage tank (ST) was a cylinder with 0.2 cm thickness, 50 cm diameter and 110 cm length but without insulation. It was opened to the outside air and used to store water pumped from the DT. The overhead tank (OT) was a cylindrical tank of 40 cm height and 30 cm diameter with an air vent (AV) above and no insulation. It had a control valve (CV) installed inside (the CV was key to make the system work automatically as shown in Fig. 2) in order to maintain 1 L of water at 30°C supplied to the DT for producing vacuum pressure. The floating ball in Fig. 2 then could move down to close a water tube when the OT water flowed to the DT. It would reopen the water tube by a buoyancy force when the pressure in the DT became to be one atmosphere. The water in the OT was refilled automatically by water from the ST or supply tank (SPT) through the floating valve. The WT was a well tank

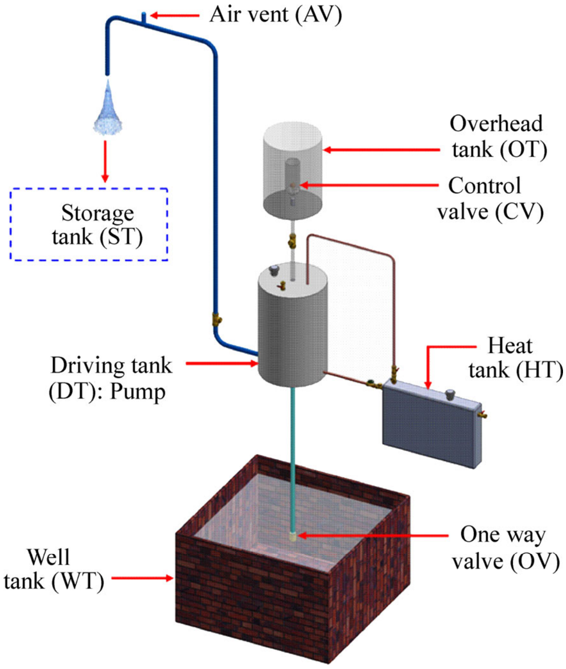

Fig. 1 Water pumping system with 10 L capacity

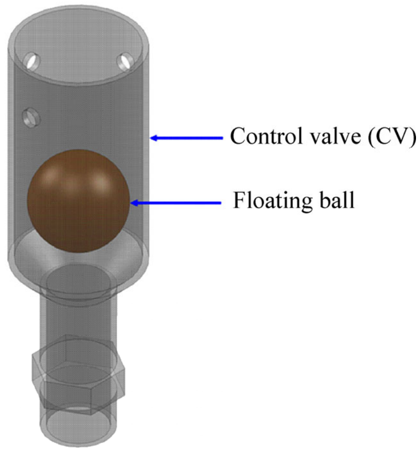

Fig. 2 Schematic diagram of CV

that stored water being pumped in the experiment. The OV was a one-way valve used to control the direction of fluid flow.

In the heat tank, the thermostat was set at 103 °C to produce vapor at 100 °C in order to ensure water boiling. All the time, a constant energy rate was supplied to a heater to produce thermal energy for the HT water. The pump had a constant 1 m discharge head. Three thousand watts heaters within the HT represented the source of waste heat as energy input for finding the suitable conditions in the experiment. In the experiment, suction head sizes varied: 2, 3.5, 5 and 6.5 m. All experimental data were recorded for 2 h at the School of Energy Environment and Materials, King Mongkut's University of Technology Thonburi. All preliminary data were recorded for every 1 s per measured data.

The vapor gage pressure inside the DT represented the pressure difference between the DT and the OT when the OT pressure was equal to one atmosphere. The pressure transducer (Cole Parmer) has ±0.25% accuracy. Seven sets of K-type thermocouples for temperature measurement were connected to a hybrid recorder (Yokogawa) with ±0.5% accuracy. HT and DT temperature values were measured by 2 points (one for air and one for water), OT temperature by 1 point and ambient temperature by 1 point. A kilowatt hour meter was used to measure the electrical energy input of the electric heater with ±2.5% accuracy. The measurement points are shown in Fig. 3.

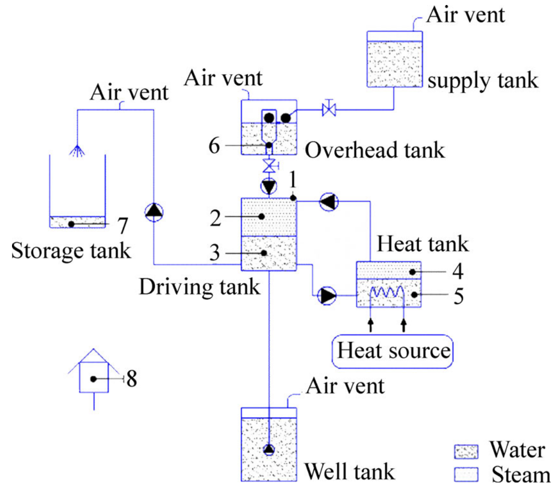

Fig. 3 Locations of temperature and pressure measurement in 10 L pump (1−Pressure of DT; 2−Steam temperature in DT; 3−Water temperature in DT; 4−Steam temperature in HT; 5−Water temperature in HT; 6−Water temperature in OT; 7−Water temperature in ST; 8−Ambient temperature)

3 System operation

3.1 Five stages

The operation of the present 10 L pump mainly consists of five stages: heating, pumping, vapor flow, cooling and suction as shown in Fig. 4.

1) Heating: During this stage, water in the HT is heated by a heater (Fig. 4(a)). The produced steam flows to the DT. The heating stage continues until the pressure in the DT is high enough to move water from the DT to the ST.

2) Pumping: When the steam pressure head in the DT is slightly more than the discharge head of the system, the DT water then is lifted upward through the discharge tube and is stored in the ST Fig. 4(a).

3) Vapor flow: After that (Fig. 4(c)), the DT steam can flow continuously to the ST.

4) Cooling: The pressure in the DT is now equal to one atmosphere. The 1 L of water in the OT at ambient temperature will flow to the DT by gravitational force. This process will cool the DT for a while.

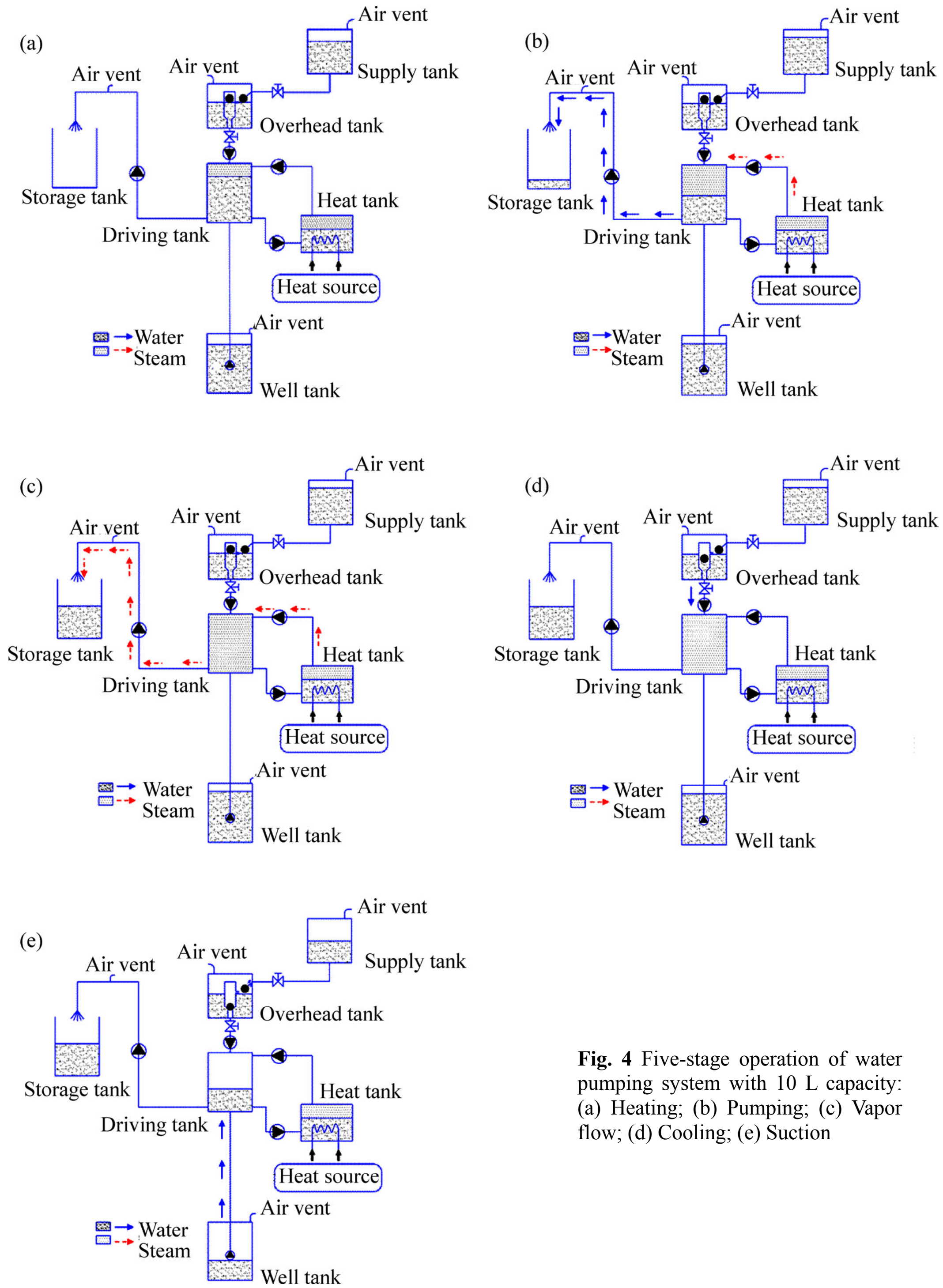

Fig. 4 Five-stage operation of water pumping system with 10 L capacity: (a) Heating; (b) Pumping; (c) Vapor flow; (d) Cooling; (e) Suction

5) Water suction: The mixing of the OT water and the DT steam creates a vacuum (Fig. 4(e)). Finally, the CV closes temporarily due to the blockage of a floating ball within the OT (Fig. 2). The 50% water and 50% air are then suctioned from the WT to the DT until the latter is full as shown in Fig. 5. The CV of the OT then opens again by buoyancy force. A pumping cycle is now complete and is ready for the subsequent cycle. The makeup water of the OT could also be obtained from the ST or SPT by siphoning if necessary.

3.2 *P*−*V* diagram of pumping process

For a clear understanding of the operation of a thermal water pump, the schematic of a pumping process is described. The change in pressure and volume in the DT (Fig. 6) of the water pumping system is presented in Fig. 7.

1) 1−2 Pumping: When the steam from the HT flows into the DT, this causes the expansion of steam within the DT. In this period, the system pumps the water inside the DT to be stored in the ST.

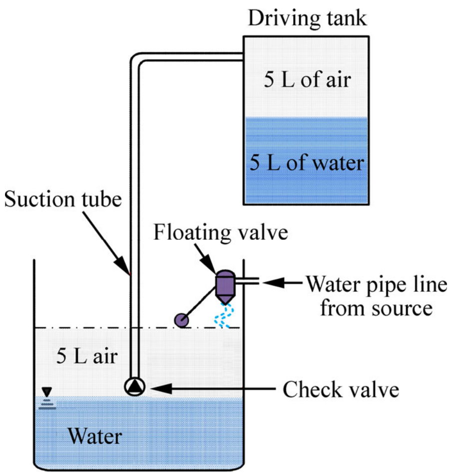

Fig. 5 Air addition to DT

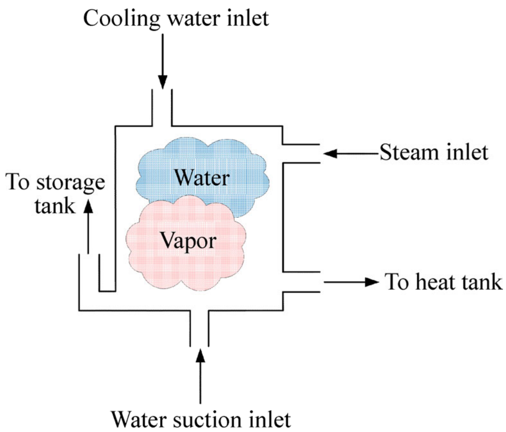

Fig. 6 Schematic diagram of fluid flow within DT

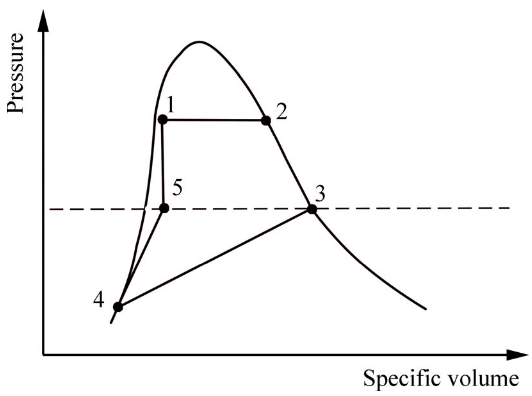

Fig. 7 *P*−*V* diagram of a pumping process

2) 2−3 Vapor flow: The water inside the DT decreases continuously by steam force until the level of the water is lower than the inlet of the discharge duct. As a result, the steam is released to the surroundings due to buoyancy effect and higher pressure. At the same time, the DT is filled with steam.

3) 3−4 Water suction: The steam in the DT is continuously released until the steam pressure inside the DT is equal to atmospheric pressure; hence, the water inside the OT flows into the DT by gravitational force. The mixing of steam and cooler water generate condensation and vacuum pressure in the DT. The steam volume suddenly decreases and suctions water from a well below to the DT.

4) 4−5 Balance pressure: The pressure inside the DT increases to one atmosphere.

5) 5−1 Heating: When the DT is fully filled by suction water from the WT, the steam produced from the HT flows into the DT again and the pressure in the DT continuously increases until the pressure in the DT is higher than the discharge head. Then, the system is ready for the next step.

4 Theoretical analysis

4.1 Heating stage

With a lumped mathematical model [17−19] being assumed, heating of HT water can be calculated by

$$Q = m_{\mathrm{w}} \times c_{\mathrm{p,w}} \times \frac{\mathrm{d}T_{\mathrm{HT}}}{\mathrm{d}t} + Q_{\mathrm{Loss}} \tag{1}$$

where Q is the thermal energy rate from heat source, m_{w} is the mass of water and steam in the HT, $c_{\mathrm{p,w}}$ is the specific heat of the water, and T_{HT} is HT water temperature.

The corresponding pressure in the HT is calculated from the perfect gas law with error ±1.6% [65]:

$$PV=mRT \tag{2}$$

where P is gas pressure, V is the volume of the tank occupied by the gas, m is the mass of the gas, R is the gas constant, and T is the temperature. Vapor pressure depends only on temperature. Gas mixture consists of air and water vapor.

The temperature that provides sufficient pressure to pump the water is around 100 °C. Pumping pressure of system is given by [64]

$$P_{\mathrm{discharge}} = (\rho_{\mathrm{w}} \times g \times h_{\mathrm{discharge}}) + P_{\mathrm{atm}} \tag{3}$$

where ρ_{w} is the water density, g is the acceleration of gravity, $h_{\mathrm{discharge}}$ is the discharge head of the system, and P_{atm} is the atmospheric pressure.

4.2 Water pumping and vapor flow stages

Water, air and steam flow to the ST are according to Bernoulli's equation [17−19]:

$$\frac{P_{\mathrm{DT}}}{\gamma} = h_{\mathrm{discharge}} + (1 + k_{\mathrm{d}})\frac{v_{\mathrm{d}}^2}{2g} \tag{4}$$

where P_{DT} is the DT gage pressure, γ is the specific weight, v_{d} is the discharge fluid velocity, k_{d} is the loss coefficient for the discharge, $h_{\mathrm{discharge}}$ is the discharge head of the system, and g is the acceleration of gravity, assuming that fluid velocity at the DT water surface is zero and is unchanged along the discharge tube.

4.3 Cooling and water suction stages

The energy balance of the mixing of the DT air-steam at 100 °C and cold water at 30 °C from the OT is shown here. The overall steam will be condensed. The cooler water is heated. Some cool water becomes saturated vapor at the mixture temperature. Therefore, the governing equation is expressed by [65]

$$m_{\mathrm{v}}(h_{\mathrm{g},100}-h_{\mathrm{f,Tmix}})+(m_{\mathrm{w}}\times c_{\mathrm{p,w}}+m_{\mathrm{a}}\times c_{\mathrm{p,a}})\cdot (100-T_{\mathrm{mix}})=m_{\mathrm{f}}(h_{\mathrm{f,Tmix}}-h_{\mathrm{f},30})+m_{\mathrm{e}}\times h_{\mathrm{fg,Tmix}} \quad (5)$$

where m_v is the steam mass in the DT at 100 °C, m_w is the pervious water mass remaining in the DT at 100 °C, m_a is the air mass in the DT at 100 °C, m_f is the water mass at 30 °C being fed to the DT, m_e is the vaporized water mass, h_g is the steam enthalpy, h_f is the water enthalpy, h_{fg} is the latent heat of vaporization, $c_{p,w}$ is the specific heat of the water, $c_{p,a}$ is the specific heat of the air, and T_{mix} is the mixing temperature.

The suction pressure of the system is given by [64]

$$P_{\mathrm{suction}}=P_{\mathrm{atm}}-(\rho_{\mathrm{w}}\times g\times h_{\mathrm{suction}}) \quad (6)$$

where ρ_w is the water density, g is the acceleration of gravity, $h_{suction}$ is the suction head of the system, and P_{atm} is the atmospheric pressure.

4.4 Pump efficiency

Mean efficiency of a pump with 10 L capacity is defined as the ratio of total hydraulic work done of a pump to total energy input during 2 h [17−19]:

$$\eta_{\mathrm{p}}=\frac{N\times W_{\mathrm{h}}}{E_{\mathrm{tot}}}\times 100\% \quad (7)$$

$$\eta_{\mathrm{p}}=f(N,\ h) \quad (8)$$

when

$$N=f(h) \quad (9)$$

$$h=h_{\mathrm{discharge}}+h_{\mathrm{suction}} \quad (10)$$

where E_{tot} is the total electrical energy input, N is the total number of the pumping cycles, and h is the overall head of the pump. W_h is the required pump hydraulic work per cycle as expressed by

$$W_{\mathrm{h}}=V_{\mathrm{c}}\times\rho_{\mathrm{w}}\times g\times h \quad (11)$$

where V_c is the pumped water volume per cycle, ρ_w is the water density, g is the acceleration of gravity, and h is the overall head of the pump.

5 Results and discussion for 10 L pump

5.1 Effect of heat input in HT

These experiments were carried out with constant 2 m suction head and 1 m discharge head. Input power was varied between 1000 and 3000 W by an electric heater inside the HT. It was found that quantity of pumped water increased with increasing input power. The input power of 3000 W could provide max amount of pumped water. Results are shown in Table 1.

Table 1 Quantity of pumped water, number of pumping cycle, energy input to an electric heater (suction head of 2 m and discharge head of 1 m)

Electrical power/W	Energy input/MJ	Number of pumping/cycle	Pumped water/L
1000	7.2	7	34
1500	10.8	17	80
2000	14.4	20	97
2500	18.0	30	145
3000	21.6	32	155

5.2 Variations in temperature and pressure of system

The pump can work automatically. The discharge head was set up and remained constant at 1 m, but the levels of suction heads were varied at 2, 3.5, 5, and 6.5 m. In the experiments, 1 L/cycle of cooling water was used for every set of conditions. The use of cooling water sped up the cooling time satisfactorily. The amount of air was 50% inside the DT.

As shown in Fig. 8, the case of 2 m suction heads shows variations of HT temperature according to Eq. (1). DT temperature and pressure were varied according to Eqs. (2)−(4). DT temperature was lower than that of HT because there were some heat losses to the outside environment and pumped water. The final steam-air-cool water mixing temperature decreased according to Eq. (5). Suction pressure also decreased according to Eqs. (2) and (5); it could be calculated by Eq. (6). It could achieve 34 pumping cycles in 2 h. The deviation of the experimental results at the suction head of 2 m is given in Table 2.

For suction heads of 3.5, 5 and 6.5 m, the numbers of pumping cycles were 23, 20 and 13, respectively. This may be due to more friction losses in longer suction tubes.

Figure 9 shows a graph of the 6.5 m suction head. It had a longer cycle period. Some cycles were not stable. The deviation of the experimental results at the suction head of 6.5 m is shown in Table 3.

5.3 Effect of air volume on pumping pressure within DT

Figure 10 shows the quantity of air relating to the generated air-steam pumping pressure within the DT when discharge head is 1 m. The supplementary air volume that could provide sufficient pumping pressure is around 5 L.

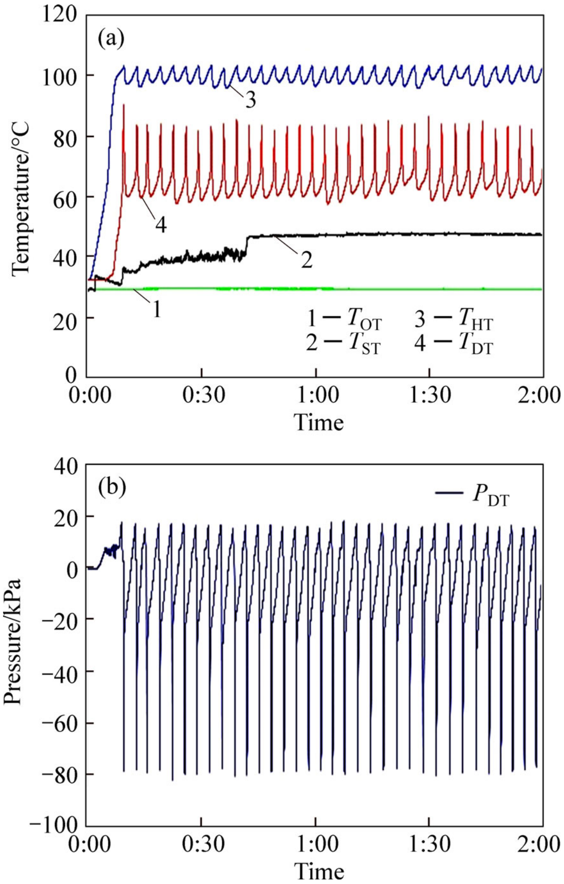

Fig. 8 Water temperature in OT (T_{OT}), mean temperature in ST (T_{ST}), mean temperature in HT (T_{HT}), mean temperature in DT (T_{DT}), gage pressure in DT (P_{DT}) as a function of time for suction head 2.0 m (10 L pump, present system): (a) Temperature; (b) Pressure

Table 2 Deviation of pressure, average temperature inside HT, average temperature in DT, average temperature in ST and temperature of OT at suction head of 2 m

Item	P_{DT}/kPa	T_{HT}/°C	T_{DT}/°C	T_{ST}/°C	T_{OT}/°C
Max	18.35	103.82	90.17	47.79	30.25
Min	−81.90	31.86	31.81	28.37	28.82
Mean	−5.53	96.55	62.15	43.35	29.50
Standard deviation	19.52	12.49	10.98	5.30	0.37

5.4 Water temperature in ST

According to the corresponding experiment, the final water temperature within the ST is approximately 43−48 °C (Fig. 11). Therefore, this water temperature is suitably high enough for residential applications.

5.5 Effect of cooling water on mixing temperature and DT suction pressure

Mixing temperature (T_{mix}) is the temperature of a mixing between steam−water in the DT at 100 °C and cooling water from the OT at 30 °C. Mixing temperature will occur before the suction stage which can be

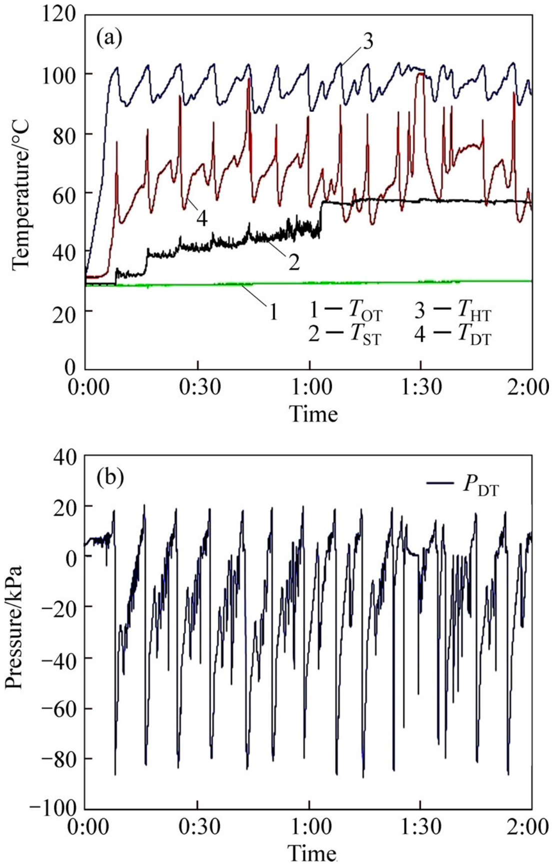

Fig. 9 Water temperature in OT (T_{OT}), mean temperature in ST (T_{ST}), mean temperature in HT (T_{HT}), mean temperature in DT (T_{DT}), gage pressure in DT (P_{DT}) as a function of time for suction head 6.5 m (10 L pump, present system): (a) Temperature; (b) Pressure

Table 3 Deviation of pressure, average temperature inside HT, average temperature in DT, average temperature in ST and temperature of OT at suction head of 6.5 m

Item	P_{DT}/kPa	T_{HT}/°C	T_{DT}/°C	T_{ST}/°C	T_{OT}/°C
Max	20.80	104.12	100.41	58.01	29.95
Min	−87.34	32.02	31.08	28.68	27.40
Mean	−15.23	94.47	63.52	49.06	29.07
Standard deviation	24.41	10.71	12.28	9.70	0.51

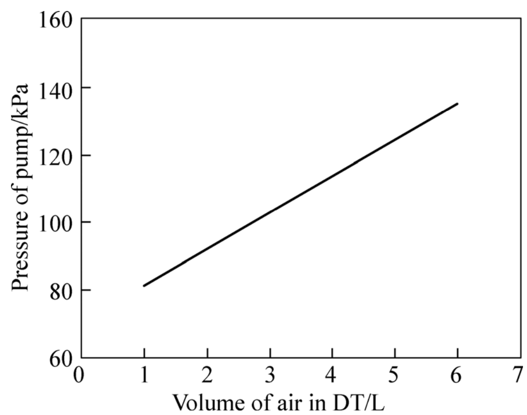

Fig. 10 Effect of air volume within DT on pumping pressure

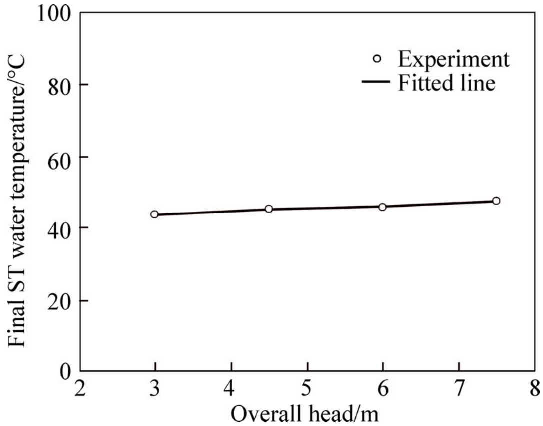

Fig. 11 Final ST water temperature from experiment as a function of overall head for 10 L pump

explained by energy-balance Eq. (5). Condensation within the DT could reduce inside pressure to a vacuum (gage pressure of −80 kPa) that could suction water from the WT into the DT until the pressure is equal to one atmosphere (gage pressure of 0 kPa). Figure 12 shows the effect of cooling water on the steam-water mixing temperature and the DT suction pressure (absolute pressure). In order to obtain the best performance, we select 1 L cooling water for the DT in each cycle.

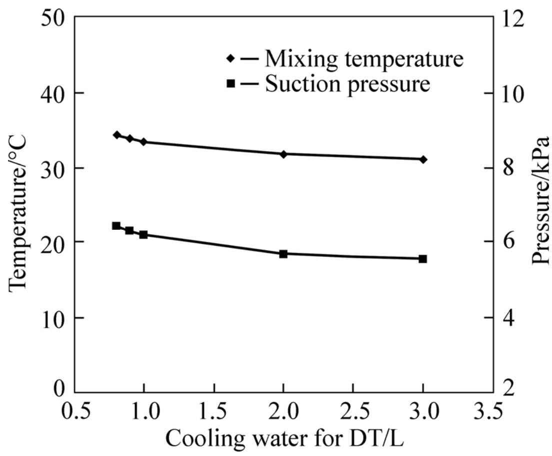

Fig. 12 Effect of a cooling water on mixing temperature and DT suction pressure

5.6 Effect length of suction tube on head loss

Figure 13 shows the relationship between the suction head and the head loss in the suction tube. It is found that the head loss will increase when the suction head increases. Equation (12) explains this relationship as [64]

$$H_{\text{loss}} = f\left(\frac{L_{\text{tube}}}{D}\right)\left(\frac{v^2}{2g}\right) \tag{12}$$

where f is friction factor of suction tube, L_{tube} is length of suction tube, D is suction tube inside diameter, v is average fluid velocity, g is the acceleration of gravity.

Fig. 13 Effect of length of suction tube on head loss

5.7 Effect of overall head on mean pump efficiency

Figure 14 shows that when the overall head increased, mean pump efficiency also increased. Evaluated from the experiment, the mean efficiencies of the water pump were equal to 0.036%, 0.035%, 0.037% and 0.021% at the overall heads of 3, 4.5, 6 and 7.5 m, respectively. An analysis of mean pump efficiency showed that mean pump efficiency was quite low according to the Carnot efficiency equation [65]:

$$\eta_{\text{Carnot}} = 1 - \frac{T_{\text{L}}}{T_{\text{H}}} \tag{13}$$

where T_{L}=303.15 K (30 °C) and T_{H}=373.15 K (100 °C).

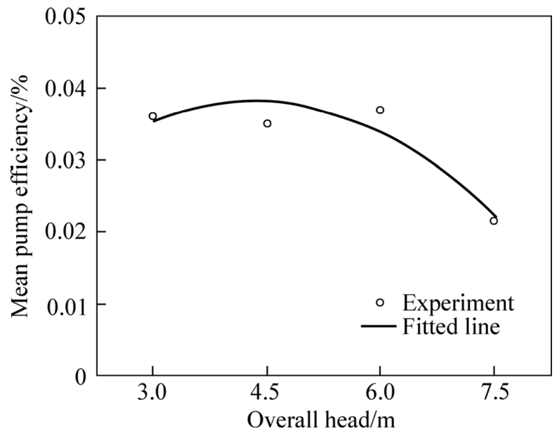

Fig. 14 Mean pump efficiency from experiment and fitted line based on Eq. (14) as a function of overall head for 10 L pump (Root-mean-square error is 0.0582%)

The high temperature (T_{H}) was too low; as a result, the mean pump efficiency was low. However, this research mainly was focused on only the amount of pumping water. The amounts of water pumped for each overall head were 170, 120, 100 and 65 L. The result of the 6.5 m suction head was not satisfactory due to high loss within the suction tube. This made the mean pump efficiency decrease.

It was concluded that the overall head has more effect on the pump efficiency than the number of pumping cycles. Based on Eqs. (7)−(11) and Fig. 15, the pump efficiency in percentage can be empirically expressed by

$$\eta_p=4.53981\times10^{-5}(-4.4667h+46.2)V_c h \quad (14)$$

when number of pumping cycle is

$$N=-4.4667h+46.2 \quad (15)$$

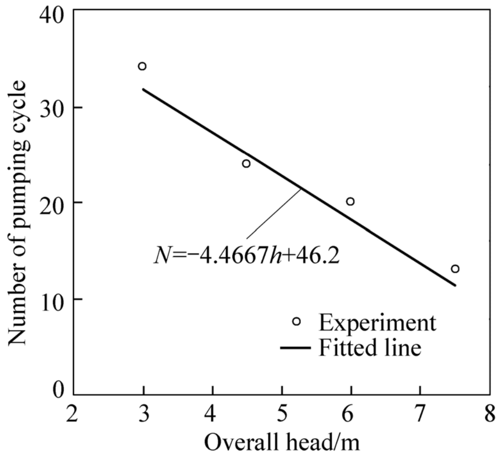

Fig. 15 Number of pumping cycle N from experiment as a function of overall head in 2 h for 10 L pump (Root-mean-square error is 6.42%)

The optimum overall head of this system was around 5 m. Moreover, the efficiency of the system was less than 1% because of heat loss in the system. Heat losses in the system were due to the following factors, heat losses from the DT to the outside, heat losses from steam to water inside the DT, and steam losses at the vapor flow stage.

Figure 14 also shows that the mean pump efficiency decreases above a certain range of the overall heads due to an increase in the energy input per cycle as well as the heating time.

5.8 Economic analysis

We compared the present 10 L pumping system and the system of von OPPEN and CHANDWALKER [66]. The estimated manufacturing cost of the present system was around 10675 baht. The economic comparison analysis is shown in Table 4. Due to free energy input, low efficiency may not be a serious drawback. Using recycled steel in pump construction could reduce cost and alleviate environmental problems.

5.9 Comparison of 10 L and Savery pumps

Table 5 shows the present 10 L capacity pump characteristics compared with a pump of the same type invented by Savery [1]. Advantage and disadvantage of both pumps were demonstrated.

5.10 Comparison of structures of 10 L and Savery pumps

Table 6 shows the structure comparison of 10 L and Savery pumps [1].

6 System operation of larger pump

The operation of a larger pump with 100−1000 L capacity is additionally explained here in detail for those who desired to use this kind of pump in practical conditions. The general operation of this system involved only three stages: heating, cooling and water suction, as shown in Fig. 16. Excluding the pumping and vapor flow stages saved more energy than that of a 10 L pump.

1) Heating stage

As presented in Fig. 16(a), valves V2 and V3 are opened while V1 and V4 are closed. The vapor gage pressure inside the tank is equal to atmospheric pressure. The water in the HT is heated and vaporized by the heat source in order to displace the inside air. The vapor flows downward through the connecting tube to the tank until the vapor temperature inside the tank reaches 97 °C, then the heat source is turned off, and the steam cools down.

2) Cooling stage

As presented in Fig. 16(b), valves V2 and V3 are closed and valve V1 is opened. After waiting for a while, the steam is cooled and 5 L of cooling water from the OT flows into the DT by gravitational force until the valve V1 is closed by a floating ball (control valve; CV in Fig. 2).

3) Water suction stage

As presented in Fig. 16(c), steam condenses into a liquid, creating a vacuum, and then the well water is sucked through the OV which is immersed in the well. Valve V4 is opened to the outside atmosphere, and valve V2 is opened to release the pumped water. After outside air displaces the water, one cycle of operation is

Table 4 Economic analysis of 10 L pump compared to system of von OPPEN and CHANDWALKER [66]

System	Lifted water/L	Suction head/m	Working fluid	Energy input	Operation time/(h·d^{-1})	Working fluid temperature/°C	Investment/Baht	Electrical energy saving/(kW·h)
von OPPEN and CHANDWALKER [66]	2000	6	Synthetic	Solar	6	40	45000	0.0385
Present system 10 L pump	1020	2	Water	Waste heat	12	90	10675	0.0654

Table 5 Advantage and disadvantage of present 10 L and Savery pumps

Present 10 L system	Savery system
1. No heat loss during steam condensation when cool water mixes with DT steam	1. Heat loss during steam condensation due to cooling by ambient air
2. Heat loss due to liquid piston	2. Heat loss due to liquid piston, which is a major loss
3. Heat loss due to steam loss at the ST during steam flow	3. During boiler is closed by a valve, it must discharge some steam to prevent explosion
4. No leak at a steam valve rod hole	4. Possible leak at a steam valve rod hole because rod frequently moves
5. Fast cooling time. A condenser is cooled when the cool water from the OT mixes with steam. This is a new cooling technique	5. Slow cooling time corresponding to item 2
6. Useful work 0.267 kJ per cycle. Required energy input 720 kJ per cycle. Ambient temperature 30 °C	6. Ambient temperature 20 °C
7. Fully automatic	7. Partially automatic, except water supply for boiler
8. Operating pressure: larger than one atmosphere	8. Operating pressure: One atmosphere
9. Working temperature: 100−103 °C	9. Working temperature: 100 °C
10. Pumped water: 5 L per cycle	10. Pumped water: 4.2 L per cycle
11. Cycle period is 4 min	11. N/A
12. Waste heat or solar energy as expected heat input	12. Solar energy as heat input

Table 6 Structure comparison of 10 L and Savery pumps

Present 10 L system	Savery system
1. HT and DT tanks made from stainless steel sheet in order to tolerate vacuum that may occur in the system	1. Pressured tank made from aluminum sheet; it comprises two semicircle pieces
2. HT tank is installed lower than DT tank in order to produce vapor pressure continually because water can be supplied to the lower tank by gravity	2. When water amount is not adequate in the boiler, some water could be suctioned into the tank automatically by vacuum pressure
3. Floating-ball valve, check valves	3. Floating-ball valve, sinking ball valve, two floaters
4. With insulation for DT and HT, heat loss may be reduced substantially	4. No insulation for boiler and condenser, so more heat loss may occur. However, it is cooled by natural convection
5. The system is small in size with an HT tank and a DT tank	5. Uses concentrated solar radiation 1 m^2 disc for heating water for vapor production
6. No moving parts: Solid piston and turbine	6. No moving parts: solid piston and turbine
7. Use of heater or other heat sources	7. Use of solar concentrator

completed.

Efficiency of a pump with large capacity in percentage excluding some losses is expressed by [1]

$$\eta_{\mathrm{p}}(\%)=\frac{V_{\mathrm{c}}\times\rho_{\mathrm{w}}\times g\times h}{(V_{\mathrm{c}}\times\rho_{\mathrm{w}}\times h_{\mathrm{fg}})+e_{\mathrm{DT}}}\times 100\% \tag{16}$$

where V_c is the pumped water volume per cycle, ρ_w is the water density at 30 °C, ρ_v is the steam density at 100 °C, g is the acceleration of gravity, h is the overall head of the system, h_{fg} is the latent heat of vaporization of water at 100 °C and e_{DT} is the energy stored by the DT shell:

$$e_{\mathrm{DT}}=(m\times c_{\mathrm{p}})_{\mathrm{DT}}\times(100-30) \tag{17}$$

where $(m\times c_p)_{DT}$ is the heat capacity of the DT. 30 °C is the initial DT temperature.

7 Results and discussion for larger pumps

7.1 Variations in temperature and pressure of 200 L pump

In an experiment with the 200 L pump and a suction head of 3 m, this system can pump around 200 L/cycle of water within 105 min. The energy input is about 6.1−

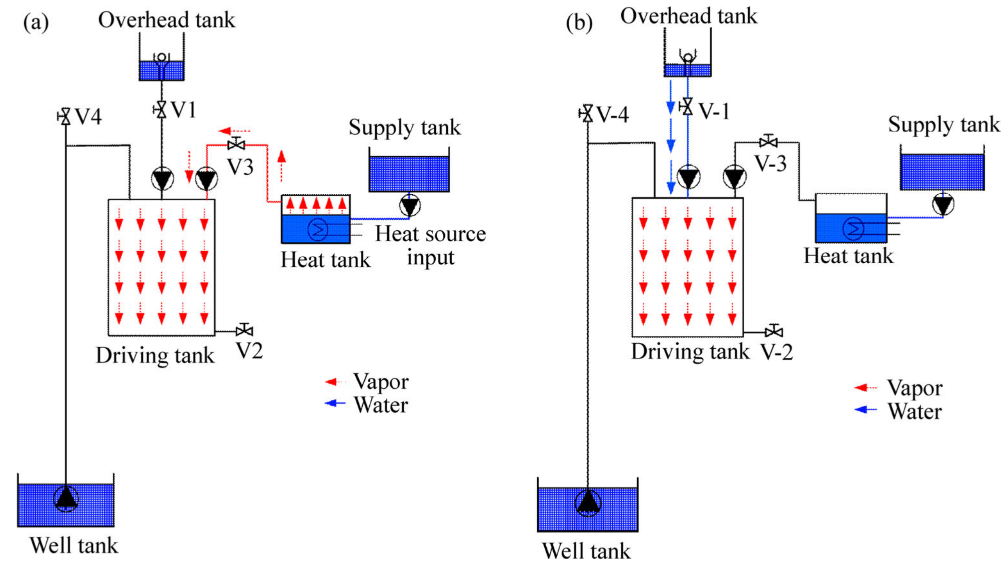

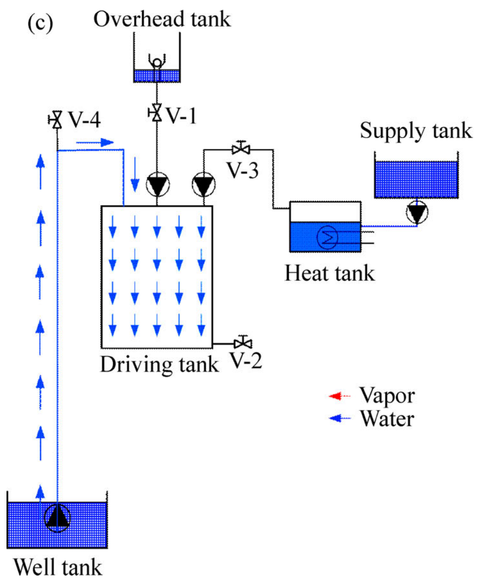

Fig. 16 Three-stage operation of large pump: (a) Heating; (b) Cooling; (c) Suction

7.5 MJ/cycle. However, in a practical condition, the quantity of output water may not be sufficient, so pumping water 2 times per day could be a better strategy. Figure 17 shows the change in temperature and pressure inside the DT. The first stage is heating within the DT. Vapor is produced from the HT and flows into the DT displacing the air inside to the outside environment, until the temperature in the DT rises to about 97 °C and then this stage is stopped. Then, the cooling stage begins by opening the CV in order to let 5 L water coolant at a temperature of 30 °C flow from the OT to mix with the high-temperature vapor in the DT by gravity. Then, vacuum occurs, and this provides the suction stage. The experimental result shows that the mixing temperature is about 32 °C and vacuum pressure is around −101.1 kPa (gage) which are different from the simulation results by 9.3% and 5%, respectively. This validates the simulation model used.

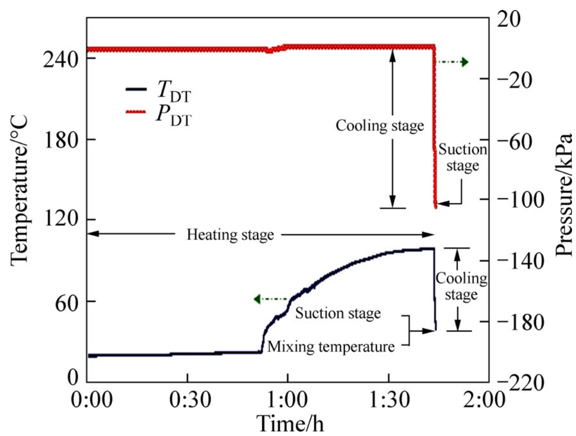

Fig. 17 Mean temperature in DT (T_{DT}) and gage pressure in DT (P_{DT}) as a function of time for suction head 3 m (200 L pump with one-cycle operation, experimental study)

7.2 Effect of mixing temperature on suction pressure

There is a mixing of cooling water and steam within the DT during the suction stage. The mixing temperature can be explained by Eq. (5) when the DT sizes were varied. Once the mixing temperature was known, the suction pressure could be evaluated. Figure 18 shows that the mixing temperature and suction pressure were nearly unchanged. However, cooling water amounts were between 1 and 40 L for the DT sizes of 100 to 1000 L, respectively (Table 7). Given suction pressure, we could estimate suction head based on Eq. (6) as shown in Fig. 19. Suction heads decreased with increasing suction pressure.

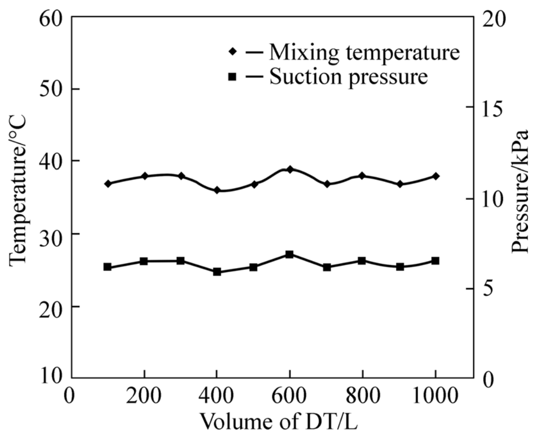

Fig. 18 Effect of DT volume on suction pressure and mixing temperature of cooling stage according to Eqs. (5)−(6)

Table 7 Effect of DT volume on cooling water volume and suction head according to Eqs. (5)−(6)

Volume of DT/L	Cooling water fed into DT/L	Suction head/m	Diameter of DT/m
100	1	9.70	0.58
200	5	9.67	0.73
300	9	9.67	0.83
400	20	9.73	0.91
500	20	9.70	0.98
600	20	9.63	1.05
700	30	9.70	1.10
800	30	9.67	1.15
900	40	9.70	1.20
1000	40	9.67	1.24

Table 8 shows the prediction of mean pump efficiency when the DT sizes were varied. According to Eqs. (16)−(17), the mean pump efficiency increased with the DT size because energy storage of the DT shell per volume (V_c) decreased when the DT size increased.

7.3 Recommendation

The temperature of thermal energy input for the thermal water pump in this work is over 100 °C. The researchers have introduced the application of thermal water pumps in residences that uses the fireplace to warm up room air, as shown in Fig. 20. The flue gas temperature is around 140−269 °C [67], which can be taken as the heat input to this thermal water pump as an example of waste heat utilization. In addition, it also helps keep the surrounding temperature of a residence reasonably low. Moreover, it is an alternative method for reducing global warming by decreasing use of fossil fuel. Another advantage of this system is that the pumped water temperature is suitably high enough for residential applications such as bathing, dishwashers, and medical use.

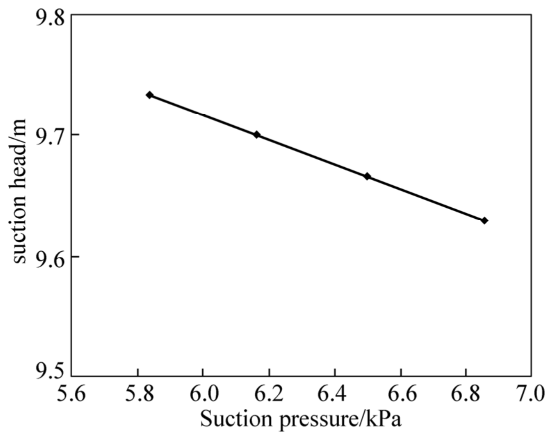

Fig. 19 Effect of suction pressure on suction head

Table 8 Effect of DT volume on large pump efficiency

Volume of DT	Mass of DT Shell, m/kg	Heat capacity of DT shell, $(m\times c_p)$/(kJ·K^{-1})	Energy stored by DT shell, $(m\times c_p\times \Delta T/V_c)$/(kJ·m^{-3})	Pump efficiency/%
100	24.69	11.96	7771.64	1.06
200	39.20	18.98	6168.36	1.28
300	51.36	24.87	5388.56	1.43
400	62.22	30.13	4895.83	1.53
500	72.20	34.96	4544.89	1.62
600	81.53	39.48	4276.90	1.70
700	90.36	43.75	4062.69	1.76
800	98.77	47.83	3885.82	1.82
900	106.84	51.73	3736.22	1.87
1000	114.61	55.50	3607.28	1.92

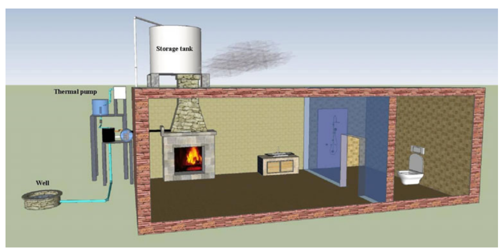

Fig. 20 Application of waste heat thermal pump in residences

8 Conclusions

1) The 10 L pumping system could pump about 65−170 L of water in 2 h, and the efficiency increases when suction increases for a certain range. After that, the efficiency decreases because of more friction loss in the suction tubes. The benefit of this system is the warm water temperature in the ST of around 43−48 °C. This system offered a new direct contact cooling technique using the mixture of low water temperature and steam within the DT in order to create a vacuum for the suction stage. This system also has other advantages, such as simple working principle, less component parts and easy construction, no moving parts compared to the solid piston pump, helps save energy by using free waste heat to produce steam, and environmentally-friendly (used water as a working fluid of the system).

2) We may use this pump to produce hot water in winter more efficiently, when supply energy is from wastes heat.

3) Economic analysis showed that the present 10 L system is comparable to the system of von OPPEN and CHANDWALKER. With the use of recycled material, this kind of pump could be more economical.

4) The researcher presents a mathematical model which is designed for the large DT suitable for practical work. The efficiency of the system increases with size of the DT.

Acknowledgements

The authors gratefully acknowledge the financial support provided by National Research Council of Thailand and the Energy Technology Division, School of Energy Environment and Materials, King Mongkut's University of Technology Thonburi. This work is also supported by the Higher Education Research Promotion and National Research University Project of Thailand, Office of the Higher Education Commission.

Nomenclature

$c_{p,\mathrm{a}}$	Specific heat of the air (kJ·(kg·K)$^{-1}$)
$c_{p,\mathrm{w}}$	Specific heat of the water (kJ·(kg·K)$^{-1}$)
D	Suction tube inside diameter (m)
E_{tot}	Total electric energy input (kJ)
e_{DT}	Energy stored by the DT shell (kJ)
f	Friction factor of suction tube (dimensionless)
g	Acceleration of gravity (9.806 m/s^2)
h	Overall head (m)
$h_{\mathrm{discharge}}$	Discharge head (m)
h_{f}	Water enthalpy (kJ/kg)
h_{fg}	Latent heat of vaporization (kJ/kg)
h_{g}	Vapor enthalpy (kJ/kg)
h_{suction}	Suction head (m)
k_{d}	Loss coefficient for discharge (dimensionless)
L_{tube}	Length of suction tube (m)
m	Mass of gas (kg)
m_{a}	Air mass (kg)
m_{v}	Mass of vapor (kg)
m_{w}	Mass of water (kg)
$(m\times c_p)_{\mathrm{DT}}$	Heat capacity of the DT (kJ·°C^{-1})
N	Total number of pumping cycle in 2 h
P	Gas pressure (kPa)
P_{atm}	Atmospheric pressure (kPa)
P_{DT}	Vapor gage pressure in the DT (kPa)
Q	Thermal energy rate from heat source (kJ)
R	Gas constant (N·m·(kg·K)$^{-1}$)
t	Time (s)
T	Temperature ($^{\circ}$C)
T_{a}	Ambient temperature ($^{\circ}$C)
T_{DT}	Mean temperature in the DT ($^{\circ}$C)
T_{HT}	Mean temperature in the HT ($^{\circ}$C)
T_{H}	High temperature ($^{\circ}$C)
T_{L}	Low temperature ($^{\circ}$C)
T_{mix}	Mixing temperature ($^{\circ}$C)
T_{OT}	Water temperature in the OT ($^{\circ}$C)
T_{ST}	Mean temperature in the ST ($^{\circ}$C)
V	Volume of tank which occupied by gas (m^3)
V_{C}	Volume of pumped water per cycle (m^3)
v	Average fluid velocity (m·s^{-1})
v_{d}	Discharge fluid velocity (m·s^{-1})
W_{h}	Required hydraulic work per cycle (kJ)
γ	Specific weight (kN·m^{-3})
ρ_{v}	Steam density (kg·m^{-3})
ρ_{w}	Water density (kg·m^{-3})
η_{p}	Mean pump efficiency (%)

Acronyms

AV	Air vent outlet
CV	Control valve
DT	Driving tank
HT	Heat tank
OT	Overhead tank
OV	One-way valve
SPT	Supply tank
ST	Storage tank
WT	Well tank

References

[1] JENNESS J R, JAMES R. Some consideration relative to a solar-powered savery water pump [J]. Solar Energy, 1961, 5: 58−60.

[2] PYTILINSKI J T. Solar energy installations for pumping irrigation water [J]. Solar Energy, 1978, 21: 255−262.

[3] BAHADORI M N. Solar water pumping [J]. Solar Energy, 1978, 21: 307−316.

[4] HIRANO S, YAMAMOTO T, TAKAMURA Y, KATSUTA M. Experimental study of downward heat pipe using principle of

heat-driven pump [C]// International Heat Pipe Symposium. Melbourne: 1996.

[5] SUDHAKAR K, KRISHNA M M, RAO D P, SOIN R S. Analysis and simulation of a solar water pump for lift irrigation [J]. Solar Energy, 1980, 24: 71−82.

[6] RAO D P, RAO K S. Solar water pump for lift irrigation [J]. Solar Energy, 1976, 18: 405−411.

[7] SHELDON J W, CRANE R A, KRANC S C. Pumping action from heat-driven oscillations in a liquid-vapour column [J]. Physics D: Applied Physics, 1976, 9: 1419−1424.

[8] PICKEN D J, SEARE K D R, GOTO F. Design and development of a water piston solar powered steam pump [J]. Solar Energy, 1997, 61: 219−224.

[9] SUMATHY K, VENKATESH A, SRIRAMULU V. The importance of the condenser in a solar water pump [J]. Energy Conversion and Management, 1995, 36: 1167−1173.

[10] SUMATHY K. Experimental studies on a solar thermal water pump [J]. Applied Thermal Engineering, 1999, 19: 449−459.

[11] WONG Y W, SUMATHY K. Performance of a solar water pump with n-pentane and ethyl ether as working fluids [J]. Energy Conversion and Management, 2000, 41: 915−927.

[12] WONG Y W, SUMATHY K. Thermodynamic analysis and optimization of a solar thermal water pump [J]. Applied Thermal Engineering, 2001, 21: 613−627.

[13] WONG Y W, SUMATHY K. Performance of a solar water pump with ethyl ether as working fluid [J]. Renewable Energy, 2001, 22: 389−394.

[14] WONG Y W, SUMATHY K. Solar thermal water pumping systems: A review [J]. Renewable and Sustainable Energy Reviews, 1999, 3: 185−217.

[15] DELGADO-TORRES A M. Solar thermal heat engines for water pumping: An update [J]. Renewable and Sustainable Energy Reviews, 2009, 13: 462−472.

[16] LIENGJINDATHAWORN S, KIRTIKARA K, NAMPRAKAI P, KIATSIRIROAT T. Parametric studies of a pulsating-steam water pump [J]. International Journal of Ambient Energy, 2002, 23(1): 37−46.

[17] ROONPRASANG N, NAMPRAKAI P, PRATINTHONG N. Experimental studies of a new solar water heater system using solar water pump [J]. Energy, 2008, 33(4): 639−646.

[18] ROONPRASANG N, NAMPRAKAI P, PRATINTHONG N. A novel thermal water pump for circulating water in a solar water heating system [J]. Applied Thermal Engineering, 2009, 29(8/9): 1598−1605.

[19] SUTTHIVIRODE K, NAMPRAKAI P, ROONPRASANG N. A new version of a solar water heating system coupled with a solar water pump [J]. Applied Energy, 2009, 86(9): 1423−1430.

[20] KOITO Y, AHAMED M S, HARADA S, IMURA H. Operational characteristics of a top-heat-type long heat transport loop through a heat exchanger [J]. Applied Thermal Engineering, 2009, 29(2/3): 259−264.

[21] CHUNG H S, WOO J S, SHIN Y H, KIM J H, JEONG H M. Experimental assessment of two-phase bubble pump for solar water heating [J]. Journal of Central South University, 2012, 19(6): 1590−1599.

[22] NAN J, JING Z, NENG Z. Energy efficiency performance of multi-energy district heating and hot water supply system [J]. Journal of Central South University, 2012, 19(5): 1377−1382.

[23] XIE J L, ZHU Q Y, XU X H. An active pipe-embedded building envelope for utilizing low-grade energy sources [J]. Journal of Central South University, 2012, 19(6): 1663−1667.

[24] CHEN J H, BAO X B, PENG Y L, YU J. Heat balance of solar-soil source heat pump compound system [J]. Journal of Central South University, 2012, 19(3): 809−815.

[25] HOSSAIN M S, SAIDUR R, FAYAZ H, RAHIM N A, ISLAM M R, AHAMED J U, RAHMAN M M. Review on solar water heater collector and thermal energy performance of circulating pipe [J]. Renewable and Sustainable Energy Reviews, 2011, 15: 3801−3812.

[26] TAO Y B, HE Y L. Numerical study on thermal energy storage performance of phase change material under non-steady-state inlet boundary [J]. Applied Energy, 2011, 88(11): 4172−4179.

[27] DOBRIANSKY Y. Concepts of self-acting circulation loops for downward heat transfer (reverse thermosiphons) [J]. Energy Conversion and Management, 2011, 52(1): 414−425.

[28] AYOMPE L M, DUFFY A, McKEEVER M, CONLON M, McCORMACK S J. Comparative field performance study of flat plate and heat pipe evacuated tube collectors (ETCs) for domestic water heating systems in a temperate climate [J]. Energy, 2011, 36(5): 3370−3378.

[29] PINEL P, CRUICKSHANK C A, BEAUSOLEIL-MORRISON I, WILLS A. A review of available methods for seasonal storage of solar thermal energy in residential applications [J]. Renewable and Sustainable Energy Reviews, 2011, 15(7): 3341−3359.

[30] DOBRIANSKY Y, DUDA M, CHLUDZINSKI D. Self-acting and self-regulating circulating pump powered by local heat instead of electricity for solar installations [C]// ISES Biennial Solar World Congress. Kassel: ISES Press, 2011: 2707−2712.

[31] PADMAVATHI K, DANIEL S A. Studies on installing solar water pumps in domestic urban sector [J]. Sustainable Cities and Society, 2011, 1(3): 135−141.

[32] XIE W T, DAI Y J, WANG R Z, SUMATHY K. Concentrated solar energy applications using Fresnel lenses: A review [J]. Renewable and Sustainable Energy Reviews, 2011, 15(6): 2588−2606.

[33] MICHAELIDES I M, ELEFTHERIOU P C. An experimental investigation of the performance boundaries of a solar water heating system [J]. Experimental Thermal and Fluid Science, 2011, 35(6): 1002−1009.

[34] CASSARD H, DENHOLM P, ONG S. Technical and economic performance of residential solar water heating in the United States [J]. Renewable and Sustainable Energy Reviews, 2011, 15(8): 3789−3800.

[35] HANAFIZADEH P, GHANBARZADEH S, SAIDI M H. Exergy analysis of airlift systems: Experimental approach [J]. International Journal of Exergy, 2011, 8(4): 407−424.

[36] HANAFIZADEH P, GHANBARZADEH S, SAIDI M H. Visual technique for detection of gas-liquid two-phase flow regime in the airlift pump [J]. Journal of Petroleum Science and Engineering, 2011, 75(3/4): 327−335.

[37] TAO Y B, HE Y L, QU Z G. Numerical study on performance of molten salt phase change thermal energy storage system with enhanced tubes [J]. Solar Energy, 2012, 86(5): 1155−1163.

[38] CHEN S W, LIU Y, HIBIKI T, ISHILL M, YOSHIDA Y, KINOSHITA I, MURASE M, MISHIMA K. Experimental study of air-water two-phase flow in an 8×8 rod bundle under pool condition for one-dimensional drift-flux analysis [J]. International Journal of Heat and Fluid Flow, 2012, 33(1): 168−181.

[39] SAHIN A Z, REHMAN S. Economical Feasibility of Utilizing Photovoltaics for Water Pumping in Saudi Arabia [J]. International Journal of Photoenergy, 2012, 2012: 542416.

[40] TYAGI V V, KAUSHIK S C, TYAGI S K. Advancement in solar photovoltaic/thermal (PV/T) hybrid collector technology [J]. Renewable and Sustainable Energy Reviews, 2012, 16(3): 1383−1398.

[41] ABU-MULAWEH H I. Design and development of solar water heating system experimental apparatus [J]. Global Journal of Engineering Education, 2012, 14(1): 99−105.

[42] CEYLAN I. Energy and exergy analyses of a temperature controlled solar water heater [J]. Energy and Buildings, 2012, 47: 630−635.

[43] PARAMESHWARAN R, KALAISELVAM S, HARIKRISHNAN S, ELAYAPERUMAL A. Sustainable thermal energy storage technologies for buildings: A review [J]. Renewable and Sustainable Energy Reviews, 2012, 16(5): 2394−2433.

[44] RODRÍGUEZ-HIDALGO M C, RODRÍGUEZ-AUMENTE P A, LECUONA A, LEGRAND M, VENTAS R. Domestic hot water consumption vs. solar thermal energy storage: The optimum size of the storage tank [J]. Applied Energy, 2012, 97: 897−906.

[45] HO C D, YEH H M, CHEN T C. Theoretical and experimental studies of the ultra-thin-channel solar water collector [J]. Heat Transfer Engineering, 2012, 33(15): 1272−1280.

[46] ABU-MULAWEH H I. Solar Water heating system experimental apparatus [C]// ASEE Annual conference and exposition. Texas: ASEE Press, 2012.

[47] TAO Y B, HE Y L, CUI F Q, LIN C H. Numerical study on coupling phase change heat transfer performance of solar dish collector [J]. Solar Energy, 2013, 90: 84−93.

[48] SHUKLA R, SUMATHY K, ERICKSON P, GONG J. Recent advances in the solar water heating systems: A review [J]. Renewable and Sustainable Energy Reviews, 2013, 19: 173−190.

[49] WANG W W, ZHANG K, WANG L B, HE Y L. Numerical study of the heat charging and discharging characteristics of a shell-and-tube phase change heat storage unit [J]. Applied Thermal Engineering, 2013, 58(1/2): 542−553.

[50] RAISUL ISLAM M, SUMATHY K, ULLAH KHAN S. Solar water heating systems and their market trends [J]. Renewable and Sustainable Energy Reviews, 2013, 17: 1−25.

[51] SHI J, SU W, ZHU M, CHEN H, PAN Y, WAN S, WANG Y. Solar water heating system integrated design in high-rise apartment in China [J]. Energy and Buildings, 2013, 58: 19−26.

[52] GOPAL C, MOHANRAJ M, CHANDRAMOHAN P, CHANDRASEKAR P. Renewable energy source water pumping systems: A literature review [J]. Renewable and Sustainable Energy Reviews, 2013, 25: 351−370.

[53] SUBIANTORO A, OOI K T. Analytical models for the computation and optimization of single and double glazing flat plate solar collectors with normal and small air gap spacing [J]. Applied Energy, 2013, 104: 392−399.

[54] LI D H W, YANG L, LAM J C. Zero energy buildings and sustainable development implications: A review [J]. Energy, 2013, 54: 1−10.

[55] FAN W, CHEN J, PAN Y, HUANG H, ARTHUR CHEN C T, CHEN Y. Experimental study on the performance of an air-lift pump for artificial upwelling [J]. Ocean Engineering, 2013, 59: 47−57.

[56] CHAN K W, McCULLOCH M. Analysis and modelling of water based bubble pump at atmospheric pressure [J]. International Journal of Refrigeration, 2013, 36(5): 1521−1528.

[57] TIGHZERT H, BRAHIMI M, KECHROUD N, BENABBAS F. Effect of submergence ratio on the liquid phase velocity, efficiency and void fraction in an air-lift pump [J]. Journal of Petroleum Science and Engineering, 2013, 110: 155−161.

[58] SETHI V P, SUMATHY K, LEE C, PAL D S. Thermal modeling aspects of solar greenhouse microclimate control: A review on heating technologies [J]. Solar Energy, 2013, 96: 56−82.

[59] CEYLAN I, ERGUN A. Thermodynamic analysis of a new design of temperature controlled parabolic trough collector [J]. Energy Conversion and Management, 2013, 74: 505−510.

[60] MENG Q, WANG C, CHEN Y, CHEN J. A simplified CFD model for air-lift artificial upwelling [J]. Ocean Engineering, 2013, 72: 267−276.

[61] YAMAGUCHAI H, ZHANG X R, NIU X D, HASHITANI N. A novel thermally driven pump and its test in a supercritical CO2 loop system [J]. International Journal of Energy Research, 2013, 37(11): 1331−1338.

[62] IBRAHIM O, FARDOUN F, YOUNES R, LOUAHLIA-GUALOUS H. Review of water-heating systems: General selection approach based on energy and environmental aspects [J]. Building and Environment, 2014, 72: 259−286.

[63] JIANG X S, JING Z X, LI Y Z, WU Q H, TANG W H. Modelling and operation optimization of an integrated energy based direct district water-heating system [J]. Energy, 2014, 64: 375−388.

[64] FOX R W, McDONALD A T. Introduction to Fluid Mechanics [R]. New York: John Wiley & Sons Inc, 2010.

[65] CENGEL Y A, BOLES M A. Thermodynamics an Engineering Approach [R]. Singapore: McGraw-Hill Companies Inc, 2006.

[66] von OPPEN M, CHANDWALKER K. Solar power for irrigation: The small solar thermal pump: an Indian development [J]. Refocus, 2001, 2(4): 24−26.

[67] PEACOCK R D. Thermal performance of masonry chimneys and fireplaces. [EB/OL].[1987]. http://fire.nist.gov/bfrlpubs/fire87/PDF/f87007.pdf.

(Edited by DENG Lü-xiang)